Reactions of Organoruthenium Phosphine Complexes with Hydroborating Reagents

R. Thomas Baker,*,† Joseph C. Calabrese,† Stephen A. Westcott,‡ and Todd B. Marder*,‡

Contribution No. 7110 from Central Research and Development, Corporate Catalysis Center, DuPont Science and Engineering Labs, Experimental Station, Wilmington, Delaware 19880-0328, and Department of Chemistry, University of Waterloo, Waterloo, Ontario, Canada N2L 3G1

Received April 5, 1995[⊗]

Abstract: In contrast to previous work on addition of E−H bonds (E = SiR_3, NR_2, OR, SR) to organoruthenium phosphine complexes, reactions of the latter with organoboranes, BRR'H, are dominated by B−C bond formation. Treatment of $RuH(PMe_3)_3(\eta^2\text{-}CH_2PMe_2)$ with thexylborane $[\{BH(CMe_2CHMe_2)(\mu\text{-}H)\}_2]$ and 9-H-BBN [9-borabicyclo-[3.3.1]nonane, $\{B(C_8H_{14})(\mu\text{-}H)\}_2$], gives ruthenaheterocycles $RuH(PMe_3)_3[\eta^1,\eta^1\text{-}PMe_2CH_2BRR'(\mu\text{-}H)]$ (**3a,b**) via insertion of B−H into the Ru−C bond. Analogous Os complexes (**3c,d**) were prepared similarly. Activation energies for exchange of M−H and M−H−B moieties in **3a−c** were estimated from ^1H and ^{31}P DNMR spectra. Benzyne complex $Ru(PMe_3)_4(\eta^2\text{-}C_6H_4)$ and thexylborane yield $Me_3P{\cdot}BH_2$(thexyl) and $Ru(PMe_3)_3[\eta^1,\eta^2\text{-}CH_2CHMeCMe_2BPh(\mu\text{-}H)_2]$ (**5**) via B−C bond formation and C−H bond activation of the thexyl side chain. Reaction of $Ru(PMe_3)_4(\eta^2\text{-}C_2H_4)$ with 9-H-BBN affords $Me_3P{\cdot}BH(C_8H_{14})$ and vinylborane complex $RuH(PMe_3)_3[\eta^2,\eta^1\text{-}CH_2{=}CHB(C_8H_{14})(\mu\text{-}H)]$ (**7**) which exists as a mixture of *fac*- and *mer*-isomers in solution. A competing pathway gives *cis*-$RuH_2(PMe_3)_4$ and 9-vinyl-BBN. These reactions provide an alternative mechanistic pathway for the metal-mediated dehydrogenative borylation of alkenes reported previously. Molecular structures of **3b,d, 5**, and *fac*-**7** were determined by X-ray diffraction.

Introduction

The discovery[1] and subsequent applications[2] of transition metal-catalyzed hydroboration of alkenes using catecholborane (HBcat, $HBO_2C_6H_4$) have rekindled interest in the interactions of organoboranes with transition metal centers.[3] While a number of examples of oxidative addition of HBcat to low valent transition metals have been reported,[4] for organoboranes, BRR'H, the only examples involve "supernucleophiles" such as $IrH(PMe_3)_4$.[5] A more common outcome of organoborane reactions involves formation of a bond between boron and the X atom of the M−X bond, where X = H, Cl, hydrocarbyl, as shown recently for phosphinorhodium complexes.[6]

The formation of vinylboronate esters in some catalyzed additions of HBcat to alkenes has elicited comparisons to similar silane-based catalysis.[2k,7] Indeed, we recently reported the first confirmed examples of alkene insertion into Rh−B bonds and of B−B bond reductive elimination.[8] The first reports of the oxidative addition of B−B bonds to low valent transition metal phosphine complexes[9,10,35] were accompanied by the discovery of catalyzed diboration of alkynes[9] and alkenes.[11] Although reactions of metal boryl ($M-BR_2$) complexes continue to contribute to our understanding of metal-catalyzed transformations of boranes,[3,8] interactions of metal hydrides and hydrocarbyls with a variety of borane reagents should provide complementary information. We report herein several reactions of alkylboranes (BRH_2 and BR'_2H) with organoruthenium phosphine complexes in which B−C bond formation predominates. Formation of vinylborane from Ru-coordinated ethylene provides an alternative mechanistic pathway for the late metal-mediated dehydrogenative borylation of alkenes.[12]

† DuPont Science and Engineering Labs.

‡ University of Waterloo.

[⊗] Abstract published in *Advance ACS Abstracts*, August 1, 1995.

(1) Männig, D.; Nöth, H. *Angew. Chem. Int. Ed. Engl.* **1985**, *24*, 878.

(2) For leading references see: (a) Burgess, K.; Ohlmeyer, M. J. *Chem. Rev.* **1991**, *91*, 1179. (b) Kocienski, P.; Jarowicki, K.; Marczak, S. *Synthesis* **1991**, 1191. (c) Westcott, S. A.; Blom, H. P.; Marder, T. B.; Baker, R. T. *J. Am. Chem. Soc.* **1992**, *114*, 8863. (d) Brands, K. M. J.; Kende, A. S. *Tetrahedron Lett.* **1992**, *33*, 5887. (e) Harrison, K. N.; Marks, T. J. *J. Am. Chem. Soc.* **1992**, *114*, 9220. (f) Gridnev, I. D.; Miyaura, N.; Suzuki, A. *Organometallics* **1993**, *12*, 589. (g) Matsumoto, Y.; Naito, M.; Uozumi, Y.; Hayashi, T. *J. Chem. Soc., Chem. Commun.* **1993**, 1468. (h) Hou, X.-L.; Hong, D.-G.; Rong, G.-B.; Guo, Y.-L.; Dai, L.-X. *Tetrahedron Lett.* **1993**, *34*, 8513. (i) Doyle, M. P.; Westrum, L. J.; Protopova, M. N.; Eismont, M. Y.; Jarstfer, M. B. *Mendeleev Comm.* **1993**, 81. (j) Evans, D. A.; Muci, A. R.; Stürmer, R.; Fu, G. C. *J. Org. Chem.* **1993**, *58*, 5307. (k) Brown, J. M.; Lloyd-Jones, G. C. *J. Am. Chem. Soc.* **1994**, *116*, 866. (l) Matthews, J. L.; Steel, P. G. *Tetrahedron Lett.* **1994**, *35*, 1421.

(3) (a) Gilbert, K. B.; Boocock, S. K.; Shore, S. G. In *Comprehensive Organometallic Chemistry*; Wilkinson, G., Stone, F. G. A., Abel, E. W., Eds.; Pergamon Press: Oxford, **1982**; Vol. 6: pp 897−914. (b) Nguyen, P.; Blom, H. P.; Westcott, S. A.; Taylor, N. J.; Marder, T. B. *J. Am. Chem. Soc.* **1993**, *115*, 9329. (c) Hartwig, J. F.; Huber, S. *J. Am. Chem. Soc.* **1993**, *115*, 4908. (d) Hartwig, J. F.; Bhandari, S.; Rablen, P. R. *J. Am. Chem. Soc.* **1994**, *116*, 1839. (e) Hartwig, J. F.; De Gala, S. R. *J. Am. Chem. Soc.* **1994**, *116*, 3661. (f) Lantero, D. R.; Motry, D. H.; Smith, M. R. 207th National ACS Meeting, San Diego, March, **1994**, Abst. INOR 38; Motry, D. H.; Smith, M. R. *J. Am. Chem. Soc.* **1995**, *117*, 6615.

(4) (a) Kono, H.; Ito, K.; Nagai, Y. *Chem. Lett.* **1975**, 1095. (b) Knorr, J. R.; Merola, J. S. *Organometallics* **1990**, *9*, 3008. (c) Westcott, S. A.; Taylor, N. J.; Marder, T. B.; Baker, R. T.; Jones, N. L.; Calabrese, J. C. *J. Chem. Soc., Chem. Commun.* **1991**, 304. (d) Westcott, S. A.; Blom, H. P.; Marder, T. B.; Baker, R. T.; Calabrese, J. C. *Inorg. Chem.* **1993**, *32*, 2175. (e) Westcott, S. A.; Marder, T. B.; Baker, R. T.; Calabrese, J. C. *Can. J. Chem.* **1993**, *71*, 930.

(5) Baker, R. T.; Ovenall, D. W.; Calabrese, J. C.; Westcott, S. A.; Taylor, N. J.; Williams, I. D.; Marder, T. B. *J. Am. Chem. Soc.* **1990**, *112*, 9399.

(6) (a) Baker, R. T.; Ovenall, D. W.; Harlow, R. L.; Westcott, S. A.; Taylor, N. J.; Marder, T. B. *Organometallics* **1990**, *9*, 3028. (b) Westcott, S. A.; Taylor, N. J.; Marder, T. B.; Baker, R. T.; Calabrese, J. C.; Harlow, R. L., submitted for publication.

(7) Westcott, S. A.; Marder, T. B.; Baker, R. T. *Organometallics* **1993**, *12*, 975.

(8) Baker, R. T.; Calabrese, J. C.; Westcott, S. A.; Nguyen, P.; Marder, T. B. *J. Am. Chem. Soc.* **1993**, *115*, 4367.

(9) Ishiyama, T.; Matsuda, N.; Miyaura, N.; Suzuki, A. *J. Am. Chem. Soc.* **1993**, *115*, 11018.

(10) Nguyen, P.; Lesley, G.; Taylor, N. J.; Marder, T. B.; Pickett, N.; Clegg, W.; Elsegood, M. R. J.; Norman, N. C. *Inorg. Chem.* **1994**, *33*, 4623.

0002-7863/95/1517-8777$09.00/0

Experimental Section

Synthesis. General details are as described previously.[2c] NMR spectra (Tables 4 and 5) were obtained using a GE Charm narrow-bore spectrometer (301 MHz ^{1}H, 121 MHz ^{31}P, 75.4 MHz ^{13}C and 96.4 MHz ^{11}B). Chemical shifts are positive downfield from external $SiMe_4$ (^{1}H, ^{13}C), 85% H_3PO_4 (^{31}P), and $BF_3{\cdot}OEt_2$ (^{11}B). Elemental analyses were performed by Mikroanalytisches Labor Pascher, Remagen, Germany. Thexylborane[13] and transition metal complexes *trans*-$RuCl_2(PMe_3)_4$,[14] *cis*-$RuH_2(PMe_3)_4$,[15] $MH(PMe_3)_3(\eta^2\text{-}CH_2PMe_2)$ (M = Ru,[16] Os[17]), $Ru(PMe_3)_4(\eta^2\text{-}C_2H_4)$,[18] and $Ru(PMe_3)_4(\eta^2\text{-}C_6H_4)$[19] were prepared as described previously, and 9-H-BBN (Aldrich) was recrystallized from hexanes before use.

Preparation of $RuH(PMe_3)_3[\eta^1,\eta^1\text{-}PMe_2CH_2BH(thexyl)(\mu\text{-}H)]$ (3a). A solution of 43 mg (0.22 mmol) of thexylborane dimer in 2 mL of hexane was added to a solution of 170 mg (0.42 mmol) of $RuH(PMe_3)_3(\eta^2\text{-}CH_2PMe_2)$ (**2a**) in 2 mL of hexane. After 20 h the solution was concentrated to 2 mL and cooled at −20 °C for 20 h to give colorless crystals of **3a**. The product was washed with 1 mL of cold (−20 °C) pentane and dried *in vacuo* to afford 174 mg of **3a** (82%): IR 2337 (B-H), 1822 cm^{-1} (Ru-H) ^{11}B NMR −11.9 ppm (br). Anal. Calcd for $C_{18}H_{51}BP_4Ru$: C, 42.95; H, 10.21; B, 2.15; P, 24.61; Ru, 20.08. Found: C, 42.60; H, 10.24; B, 2.14; P, 24.2; Ru, 19.1.

The Os analogue **3c** was generated in toluene-d_8 solution from 2 equiv of $OsH(PMe_3)_3(\eta\text{-}CH_2PMe_2)$ (**2b**) and 1.1 equiv of thexylborane dimer. The resulting solution was characterized by multinuclear NMR spectroscopy (Tables 4 and 5): ^{11}B NMR −9.3 ppm (br).

The 9-BBN analogues, **3b,d** were prepared similarly from 30 mg (0.12 mmol) of 9-H-BBN dimer and 0.21 mmol of the metal complex (85 mg of **2a** or 104 mg of **2b**) in 2 mL of hexane to give 90 mg of **3b** (81%) and 95 mg of **3d** (73%). For **3b**: IR 1856 cm^{-1} (Ru-H); ^{11}B NMR 0.4 ppm (br). Anal. Calcd for $C_{20}H_{51}BP_4Ru$: C, 45.55; H, 9.75; B, 2.05; P, 23.49; Ru, 19.16. Found: C, 45.18; H, 9.76; B, 2.03; P, 23.2; Ru, 18.0. For **3d**: IR 1932 cm^{-1} (Os-H); ^{11}B NMR 5.7 ppm (br). Anal. Calcd for $C_{20}H_{51}BOsP_4$: C, 38.96; H, 8.34; B, 1.75; Os, 30.85; P, 20.1. Found: C, 38.55; H, 8.33; B, 1.70; Os, 30.4; P, 19.7.

Preparation of $Ru(PMe_3)_3[\eta^1,\eta^2\text{-}CH_2CHMeCMe_2BPh(\mu\text{-}H)_2]$ (5). A solution of 60 mg (0.31 mmol) of thexylborane dimer in 2 mL of hexane was added to a solution of 144 mg (0.30 mmol) of $Ru(PMe_3)_4(\eta^2\text{-}C_6H_4)$ (**4**) in 5 mL of toluene. After 20 h, the solvent was removed *in vacuo*, and the residue was dissolved in hexane. After cooling the orange solution at −20 °C for 2 days, the resulting yellow crystals were collected by filtration, washed with 2 mL of cold (−80 °C) pentane, and dried *in vacuo* to yield 112 mg of **5** (74%): ^{11}B{^{1}H} NMR −12.4 ppm (br); ^{13}C{^{1}H} NMR (THF-d_8) 150.7 (v br, ipso of Ph), 133.2 (br, 2C, ortho of Ph), 126.6 (2C, meta of Ph), 125.0 (para of Ph), 53.5 (*C*HMe), 37.9 (Br, *C*Me$_2$), 34.0 (d tr, $^2J_{CP}$ = 59, 9 Hz, *C*H$_2$), 28.0 (s, CH*Me*), 24.4 (d, 3C, J_{CP} = 20 Hz, PMe$_3$), 23.2 (d, 3C, J_{CP} = 28 Hz, PMe$_3$), 22.6 (d, 3C, J_{CP} = 28 Hz, PMe$_3$), 20.8, 17.3 (s, *C*Me$_2$). Anal. Calcd for $C_{21}H_{46}BP_3Ru$: C, 50.11; H, 9.21; B, 2.15; P, 18.46; Ru, 20.08. Found: C, 50.33; H, 9.33; B, 2.32; P, 17.8; Ru, 18.9.

Preparation of $RuH(PMe_3)_3[\eta^2,\eta^1\text{-}CH_2{=}CHB(C_8H_{14})(\mu\text{-}H)]$ (7). A solution of 170 mg (0.7 mmol) of 9-H-BBN dimer in 5 mL of toluene was added slowly to a solution of 305 mg (0.7 mmol) of $Ru(PMe_3)_4(\eta^2\text{-}C_2H_4)$ (**6**) in 10 mL of hexane cooled to −80 °C. After warming to 25 °C and stirring for 18 h, the solvent was removed *in vacuo*, and the residue was triturated with cold (−20 °C) hexane and filtered to remove $Me_3P{\cdot}BH(C_8H_{14})$. The filtrate was cooled at −20 °C for 18 h, and the resulting pale yellow crystals were collected by filtration, washed with 2 mL of cold (−80 °C) pentane, and dried *in vacuo* to give 165 mg of **7** (49%). Complex **7** was recrystallized from toluene/hexane 1:2 at −20 °C: spectroscopic data for *fac*-**7** IR (Nujol) 1899 cm^{-1} (Ru-H); ^{11}B NMR −5.0 ppm (br); ^{13}C{^{1}H} NMR 79.6 (br, B*C*H=CH$_2$), 52.7 (d, $^2J_{CP}$ = 12 Hz, BCH=*C*H$_2$). For *mer*-**7** IR (hexane) 1910 cm^{-1} (Ru-H); ^{11}B NMR −5.0 ppm (br); ^{13}C{^{1}H} NMR (THF-d_8) 81.2 (br, B*C*H=CH$_2$), 59.5 (s, BCH=*C*H$_2$). Anal. Calcd for $C_{19}H_{46}BP_3Ru$: C, 47.61; H, 9.67; B, 2.26; P, 19.38; Ru, 21.08. Found: C, 47.47; H, 9.77; B, 2.18; P, 19.0; Ru, 19.7.

Molecular Structure Determination. Crystals suitable for X-ray diffraction were obtained as described above. A summary of the crystallographic results is presented in Table 1. All data sets were collected at low temperature on Enraf-Nonius CAD4 or Syntex R3 diffractometers using graphite-filtered Mo radiation. Data were reduced in the usual fashion for Lorentz-polarization, and azimuthal absorption corrections were applied for **3b,d** and **5** (range of transmission factors = 0.81−0.86, 0.25−0.33, and 0.76−0.79, respectively). Structure solution and refinement were performed on a VAX/IBM cluster system using a local program set. The structure of **3b** was solved by direct methods (SHELX),[20] while for **3d**, **5**, and **7** heavy atom positions were obtained via automated Patterson analysis and used to phase reflections for the remaining light atoms via the usual combination of structure factor, Fourier synthesis, and full-matrix least-squares refinement. All refinements were performed using full-matrix least squares on F, with anisotropic thermal parameters for all non-hydrogen atoms, and included anomalous dispersion terms[21] for Ru, Os, and P as well as idealized hydrogen coordinates as fixed atom contributors. The data were of sufficient quality that all hydrogens were refined successfully with the exception of the C5 and C6 methyl hydrogens in **5**; thus only the Ru−H−B hydrogens were varied in the final model of **5**, and the largest residual electron density was 1.63e/Å^3, near C3. The atomic scattering factors were taken from the tabulations of Cromer and Waber.[22] For **5** and **7** the asymmetric unit consists of one molecule in a general position. Selected bond distances and angles for **3b,d**, **5**, and **7** are given in Tables 2, 3, 7, and 8. Tables of final positional and thermal parameters for non-hydrogen atoms, general temperature factors, and hydrogen atom positions are available as supporting information.

Results

In contrast to the d^8 hydridorhodium and -iridium phosphine complexes reported previously,[5,6] the d^6 dihydride complexes *cis*-$MH_2(PMe_3)_4$ (**1**, M = Ru, Os) do not react readily with thexylborane $[\{BH(CMe_2CHMe_2)(\mu\text{-}H)\}_2]$ and 9-H-BBN (9-borabicyclo[3.3.1]nonane, $[B(C_8H_{14})(\mu\text{-}H)]_2$) at ambient temperature. Reactions of monohydride $RuH(PMe_3)_3(\eta^2\text{-}CH_2PMe_2)$ (**2a**) with these boranes, however, gave colorless crystals of the new ruthenaheterocycles $RuH(PMe_3)_3[\eta^1,\eta^1\text{-}PMe_2CH_2BRR'(\mu\text{-}H)]$ (**3a,b**). Complexes **3a,b** were characterized by elemental

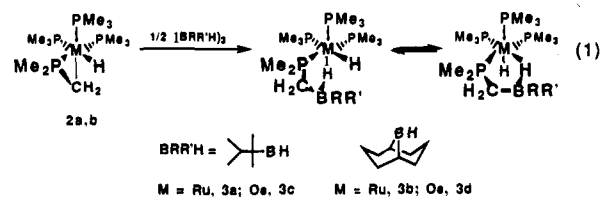

(1)

analysis, IR, and multinuclear NMR spectroscopy, and the molecular structure of **3b** was determined by single crystal X-ray diffraction. The analogous osmium complexes **3c,d** were

(11) Baker, R. T.; Nguyen, P.; Marder, T. B.; Westcott, S. A. *Angew. Chem., Int. Ed. Engl.* **1995**, *34*, 1336.
(12) Presented in part at the 200th National ACS meeting, Washington, August, **1990**, Abst. INOR 429.
(13) Pelter, A.; Smith, K.; Brown, H. C. *Borane Reagents*; Academic Press: New York, 1988.
(14) Sellmann, D.; Bohlen, E. *Z. Naturforsch., Anorg. Chem., Org. Chem.* **1982**, *37*, 1026.
(15) Jones, R. A.; Wilkinson, G.; Colquohoun, I. J.; McFarlane, W.; Galas, A. M. R.; Hursthouse, M. B. *J. Chem. Soc., Dalton Trans.* **1980**, 2480.
(16) Werner, H.; Werner, R. *J. Organomet. Chem.* **1981**, *209*, C60.
(17) Werner, H.; Gotzig, J. *Organometallics* **1983**, *2*, 547.
(18) Wong, W.-K.; Chiu, K. W.; Statler, J. A.; Wilkinson, G.; Motavelli, M.; Hursthouse, M. B. *Polyhedron* **1984**, *3*, 1255.
(19) Hartwig, J. F.; Bergman, R. G.; Andersen, R. A. *J. Am. Chem. Soc.* **1991**, *113*, 3404.
(20) Sheldrick, G. M. *SHELX*, University of Gottingen, Federal Republic of Germany, 1986.
(21) Cromer, D. T.; Ibers, J. A. *International Tables for X-ray Crystallography*; Kynoch Press: Birmingham, England, 1974; Vol. IV, Table 2.31.
(22) Cromer, D. T.; Waber, J. T. *International Tables for X-ray Crystallography*; Kynoch Press: Birmingham, England, 1974; Vol. IV, Table 2.2A.

Table 1. Summary of X-ray Diffraction Data

complex	$RuH(PMe_3)_3[PMe_2CH_2BH(C_8H_{14})]$ (**3b**)	$OsH(PMe_3)_3[PMe_2CH_2BH(C_8H_{14})]$ (**3d**)	$Ru(PMe_3)_3[CH_2CHMeCMe_2BH_2Ph]$ (**5**)	$RuH(PMe_3)_3[CH_2{=}CHBH(C_8H_{14})]$ (**7**)
formula	$C_{20}H_{51}BP_4Ru$	$C_{20}H_{51}BOsP_4$	$C_{21}H_{46}BP_3Ru$	$C_{19}H_{46}BP_3Ru$
fw	527.43	616.53	503.43	479.41
a, Å	15.328(2)	15.300(3)	10.059(2)	14.669(3)
b, Å	9.841(2)	9.798(2)	10.378(2)	17.951(4)
c, Å	19.542(4)	19.534(3)	14.998(3)	18.667(2)
α, deg	90	90	74.71(2)	90
β, deg	112.75(1)	112.83(1)	82.22(2)	90
γ, deg	90	90	61.52(2)	90
v, Å^3	2718.4	2698.9	1327.4	4915.5
Z	4	4	2	8
ϱ_{calcd}, g cm^{-3}	1.288	1.517	1.259	1.295
space group	$P2_1/c$ (no. 14)	$P2_1/c$ (no. 14)	$P\bar{1}$ (no. 2)	*Pbca* (no. 61)
cryst dimens, mm	0.30 × 0.14 × 0.36	0.28 × 0.20 × 0.30	0.37 × 0.32 × 0.46	0.35 × 0.23 × 0.50
temp, °C	−100	−100	−70	−70
radiation	Mo Kα	Mo Kα	Mo Kα	Mo Kα
μ, cm^{-1}	8.02	49.69	7.61	8.19
data collection method	*ω*-2*θ*	*ω*-2*θ*	*ω*-2*θ*	*ω*-2*θ*
max 2*θ*, deg	55.0	55.0	55.0	55.0
scan speed, deg/min	3.90−11.70	3.90−11.70	1.70−5.00	1.70−5.00
scan width, deg	1.00*ω*	1.20*ω*	1.20−1.90*ω*	1.20−1.90*ω*
total no. of observns	6798	6807	6294	6206
no. of unique data, $I > 3\sigma(I)$	4725	5033	4986	3750
final no. of variables	439	439	243	401
final max. shift/error	0.03	0.15	0.04	0.05
max. residual density, e$^-$/Å^3	0.47	0.52	1.63	0.35
R^a	0.027	0.021	0.031	0.028
$R_w{}^b$	0.034	0.021	0.034	0.025

^{a} $\sum||F_o| - |F_c||/\sum|F_o|$. ^{b} $[\sum w(|F_o| - |F_c|)^2/\sum wF_o^2]^{1/2}$.

Table 2. Selected Bond Distances (Å) and Angles (deg) for $RuH(PMe_3)_3[\eta^1,\eta^1\text{-}PMe_2CH_2B(C_8H_{14})(\mu\text{-}H)]$ (**3b**)

Ru(1)−P(1)	2.3217 (8)	P(1)−Ru(1)−P(2)	97.03 (3)
Ru(1)−P(2)	2.3541 (8)	P(1)−Ru(1)−P(3)	159.53 (4)
Ru(1)−P(3)	2.3331 (8)	P(1)−Ru(1)−P(4)	97.76 (3)
Ru(1)−P(4)	2.2576 (9)	P(2)−Ru(1)−P(3)	99.00 (3)
Ru(1)−H(1B)	1.941 (21)	P(2)−Ru(1)−P(4)	96.80 (3)
Ru(1)−H(1RU)	1.568 (37)	P(3)−Ru(1)−P(4)	92.91(3)
P(1)−C(11)	1.807 (3)	P(1)−Ru(1)−H(1B)	80.9 (6)
P(1)−C(12)	1.826 (4)	P(1)−Ru(1)−H(1RU)	77 (1)
P(1)−C(13)	1.827 (4)	P(2)−Ru(1)−H(1B)	87.7 (6)
P(2)−C(21)	1.828 (4)	P(2)−Ru(1)−H(1RU)	173 (1)
P(2)−C(22)	1.834 (4)	P(3)−Ru(1)−H(1B)	87.1 (6)
P(2)−C(23)	1.829(4)	P(3)−Ru(1)−H(1RU)	86 (1)
P(3)−C(31)	1.827 (4)	P(4)−Ru(1)−H(1B)	175.5 (6)
P(3)−C(32)	1.843 (3)	P(4)−Ru(1)−H(1RU)	87 (1)
P(3)−C(33)	1.835 (4)	H(1B)−Ru(1)−H(1RU)	88 (1)
P(4)−C(41)	1.829 (4)	Ru(1)−P(1)−C(11)	102.7 (1)
P(4)−C(42)	1.828 (4)	Ru(1)−P(1)−C(12)	116.7 (1)
P(4)−C(43)	1.820 (4)	Ru(1)−P(1)−C(13)	127.3 (1)
C(1)−C(2)	1.545 (4)	Ru(1)−P(2)−C(21)	116.2 (1)
C(1)−C(8)	1.522 (5)	Ru(1)−P(2)−C(22)	119.8 (1)
C(2)−C(3)	1.527 (5)	Ru(1)−P(2)−C(23)	119.9 (1)
C(3)−C(4)	1.539 (5)	Ru(1)−P(3)−C(31)	117.6 (1)
C(4)−C(5)	1.548 (4)	Ru(1)−P(3)−C(32)	123.6 (1)
C(5)−C(6)	1.533 (5)	Ru(1)−P(3)−C(33)	115.1 (1)
C(6)−C(7)	1.542 (5)	Ru(1)−P(4)−C(41)	119.1 (2)
C(7)−C(8)	1.533 (6)	Ru(1)−P(4)−C(42)	120.6 (1)
C(1)−B(1)	1.620 (5)	Ru(1)−P(4)−C(43)	116.4 (1)
C(5)−B(1)	1.615 (5)	C(11)−P(1)−C(12)	104.4 (2)
C(11)−B(1)	1.639 (5)	C(11)−P(1)−C(13)	103.8 (2)
B(1)−H(1B)	1.367 (21)	P(1)−C(11)−B(1)	107.0 (2)
Ru(1)−B(1)	2.994 (1)	C(1)−B(1)−C(5)	105.7 (3)
		C(1)−B(1)−C(11)	113.8 (3)
		C(5)−B(1)−C(11)	116.7 (3)
		C(1)−B(1)−H(1B)	101 (1)
		C(5)−B(1)−H(1B)	111 (1)
		C(11)−B(1)−H(1B)	107 (1)
		Ru(1)−H(1B)−B(1)	129 (1)

Table 3. Selected Bond Distances (Å) and Angles (deg) for $OsH(PMe_3)_3[\eta^1,\eta^1\text{-}PMe_2CH_2B(C_8H_{14})(\mu\text{-}H)]$ (**3d**)

Os(1)−P(1)	2.3287 (8)	P(1)−Os(1)−P(2)	96.76 (3)
Os(1)−P(2)	2.3375 (8)	P(1)−Os(1)−P(3)	159.77 (3)
Os(1)−P(3)	2.3298 (8)	P(1)−Os(1)−P(4)	97.82 (3)
Os(1)−P(4)	2.2657 (8)	P(2)−Os(1)−P(3)	98.85 (3)
Os(1)−H(1B)	1.841 (33)	P(2)−Os(1)−P(4)	96.51 (3)
Os(1)−H(1OS)	1.617 (34)	P(3)−Os(1)−P(4)	93.11 (3)
P(1)−C(11)	1.803 (3)	P(1)−Os(1)−H(1B)	80 (1)
P(1)−C(12)	1.826 (3)	P(1)−Os(1)−H(1OS)	79 (1)
P(1)−C(13)	1.830 (4)	P(2)−Os(1)−H(1B)	88 (1)
P(2)−C(21)	1.825 (4)	P(2)−Os(1)−H(1OS)	175 (1)
P(2)−C(22)	1.833 (4)	P(3)−Os(1)−H(1B)	88 (1)
P(2)−C(23)	1.826 (4)	P(3)−Os(1)−H(1OS)	85 (1)
P(3)−C(31)	1.828 (3)	P(4)−Os(1)−H(1B)	175 (1)
P(3)−C(32)	1.847 (4)	P(4)−Os(1)−H(1OS)	86 (1)
P(3)−C(33)	1.833 (3)	H(1B)−Os(1)−H(1OS)	89 (2)
P(4)−C(41)	1.824 (4)	Os(1)−P(1)−C(11)	103.5 (1)
P(4)−C(42)	1.830 (4)	Os(1)−P(1)−C(12)	116.3 (1)
P(4)−C(43)	1.827 (4)	Os(1)−P(1)−C(13)	126.6 (1)
C(1)−C(2)	1.543 (4)	Os(1)−P(2)−C(21)	116.7 (1)
C(1)−C(8)	1.535 (5)	Os(1)−P(2)−C(22)	119.8 (1)
C(2)−C(3)	1.525 (5)	Os(1)−P(2)−C(23)	119.8 (1)
C(3)−C(4)	1.536 (5)	Os(1)−P(3)−C(31)	118.0 (1)
C(4)−C(5)	1.549 (5)	Os(1)−P(3)−C(32)	123.1 (1)
C(5)−C(6)	1.536 (5)	Os(1)−P(3)−C(33)	114.8 (1)
C(6)−C(7)	1.530 (5)	Os(1)−P(4)−C(41)	119.2 (1)
C(7)−C(8)	1.524 (5)	Os(1)−P(4)−C(42)	121.0 (1)
C(1)−B(1)	1.612 (4)	Os(1)−P(4)−C(43)	115.9 (1)
C(5)−B(1)	1.605 (4)	C(11)−P(1)−C(12)	105.0 (2)
C(11)−B(1)	1.636 (4)	C(11)−P(1)−C(13)	103.8 (2)
B(1)−H(1B)	1.428 (33)	P(1)−C(11)−B(1)	106.6 (2)
		C(1)−B(1)−C(5)	106.6 (2)
		C(1)−B(1)−C(11)	114.0 (3)
		C(5)−B(1)−C(11)	117.1 (3)
		C(1)−B(1)−H(1B)	104 (1)
		C(5)−B(1)−H(1B)	110 (1)
		C(11)−B(1)−H(1B)	105 (1)
		Os(1)−H(1B)−B(1)	133 (2)

prepared similarly and characterized spectroscopically (**3d** by X-ray diffraction).

The molecular structure of **3b** (Figure 1) consists of a pseudooctahedral ruthenium center with meridional PMe_3 ligands and *cis* hydride and Ru−H−B moieties. Formal insertion of the B−H bond of the organoborane into the Ru−C bond of the metalated phosphine thus affords a novel Ru−H−B−C−P metallaheterocycle which is nearly planar. Crystals

Table 4. ^{1}H NMR Spectra[a]

compd	M−H	M−H−B	PMe_3	other
3a	−8.5 (br d, 80)	−12.0 (br s)	1.44 (d d, 7, 1.5, 9H), 1.37 (br, 18H)	1.37 (br ov, P*Me*$_2$), 1.15 (br s, PC*H*$_2$), 0.76 (d, 7, CH*Me*$_2$), 0.68 (s, C*Me*$_2$)
at −90 °C[b]	−8.4 (d q, 84, 26)	−12.0 (br d, 26)	1.42 (d, **7**), 1.39 (d, 6), 1.29 (d, 8)	1.12 (br s, PC*H*$_2$), 0.94 (mult, PC*H*$_2$), 0.73 (d, 11, 3H, CH*Me*$_2$), 0.71 (d, 12, 3H, CH*Me*$_2$), 0.68, 0.63 (s, C*Me*$_2$), PMe_2 doublets obscured
3b	−9.85 (mult)		1.46 (d d, 7, 2, 9H), 1.35 (d, 6.5, 18H)	1.43 (d d, 8, 2, P*Me*$_2$), 0.76 (br s, PC*H*$_2$)
at −80 °C[b]	−7.80 (d q, 84, 25)	−11.56 (br d, 37)	1.35 (d, 6.5), 1.31 (d, 6), 1.20 (d, 7)	1.26 (d, 7, 3H, P*Me*$_2$), 1.45 (d, 8, 3H, P*Me*$_2$), 0.79, 0.41 (br s, PC*H*$_2$)
3c	−9.5 (br)	−13.2 (br)	na[c]	na[c]
at −80 °C[b]	−9.35 (d q, 60.5, 15)	−13.75 (br d, 23)	na[c]	na[c]
3d	−10.78 (br mult)		na[c]	na[c]
at −80 °C[b]	−8.72 (d q, 60, 20)	−13.22 (br d, 25)	na[c]	na[c]
5		−8.22, −8.70 (br)	1.42 (d, 8), 1.34 (d, 8.5), 1.02 (d, 5.5)	7.13 (mult, 2H, ortho), 7.07 (tr, 8, 2H, meta), 6.96 (mult, para), 1.4 (ov mult, 2H, C*H*$_2$), 1.02 (mult, C*H*Me), 0.88 (d, 6.5, 3H, CH*Me*), 0.49, 0.42 (s, 3H, C*Me*$_2$)
fac-**7**	−10.60 (d tr, 69, 28)	−13.30 (d, 56)	1.85 (d, 8.5), 1.67 (d, 5.5), 1.50 (d, 7.5)	4.62 (tr, 11, =C*H*), 2.69 (br mult, =C*H*), 2.45 (tr, 14, =C*H*)
mer-**7**	−8.84 (tr d, 34, 19)	−12.04 (br d, 42)	1.88 (ov mult, 18H), 1.73 (d, 5)	3.73 (d tr, 13, 10, =C*H*), 3.15 (tr, 8.5, =C*H*), 3.09 (tr d, 14, 3, =C*H*)

[a] Recorded at 25 °C in toluene-d_8; multiplicity, J_{HP}, J_{HH} in parentheses. [b] Recorded in THF-d_8. [c] Not assigned.

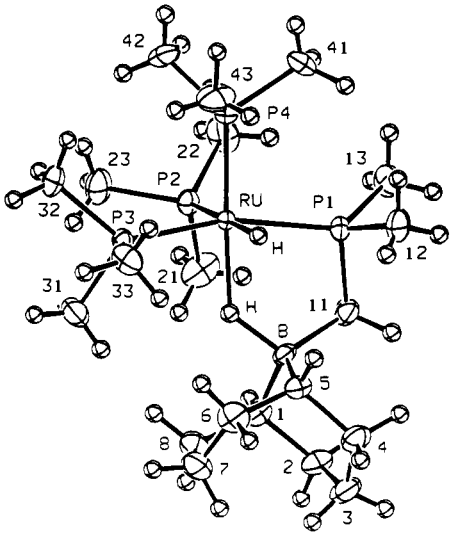

Figure 1. Molecular structure of RuH(PMe_3)$_3$[η^1,η^1-PMe_2CH_2B-(C_8H_{14})(μ-H)] (**3b**).

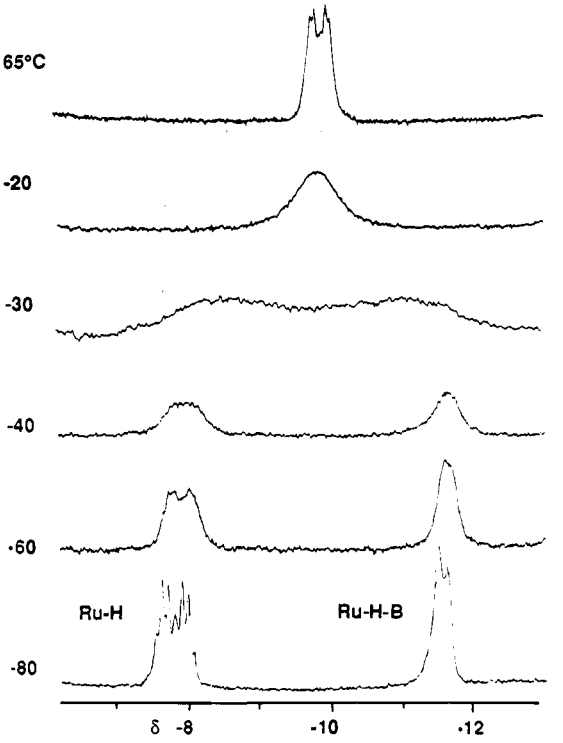

Figure 2. ^{1}H DNMR spectra of RuH(PMe_3)$_3$[η^1,η^1-$PMe_2CH_2B(C_8H_{14})$-(μ-H)] (**3b**).

of the Os analogue **3d** are isomorphous with those of **3b** and the molecular structure is very similar (Tables 2 and 3). The Ru−P1,P3 distances (av 2.327(1) Å) are typical for mutually *trans* ligands as found in *cis*-RuHX(PMe_3)$_4$ (Ru−P_{av} = 2.328-(2) Å for both X = O-*p*-tol and NHPh),[23] as is Ru−P2 *trans* to H (2.354(1) vs 2.364(2) Å for *cis*-RuHX(PMe_3)$_4$). The Ru−P4 distance (2.258(1) Å) is significantly shorter, reflecting the weak *trans* influence of the substituted borohydride (cf. Ru−P = 2.259(3) Å in *mer*-RuH(η^2-H_2BH_2)(PMe_3)$_3$.[24]

Complexes **3a**−**d** are fluxional as a result of exchange between Ru−H and Ru−H−B as shown in the ^{1}H DNMR spectra of **3b** (Table 4, Figure 2). The corresponding ^{31}P NMR spectra are particularly informative as exchange is observed only for the PMe_3 ligands trans to hydride and to the Ru−H−B bridge (Table 5, Figure 3). The activation energies $\Delta G^{\ddagger}_{Tc}$ for this exchange process were estimated from the DNMR spectra (Table 6) to be 14.7, 10.5, and 13.0 ± 0.3 kcal/mol for **3a**−**c**, respectively.

Reaction of the benzyne complex Ru(PMe_3)$_4$(η^2-C_6H_4) (**4**) with 1 equiv of thexylborane dimer yielded 1 equiv of $Me_3P{\cdot}BH_2$(thexyl) and colorless crystals of Ru(PMe_3)$_3$[η^1,η^2-$CH_2CHMeCMe_2BPh(\mu\text{-}H)_2$] (**5**, eq 2). Similar reactions of **4** and 9-H-BBN gave a mixture of products which was not

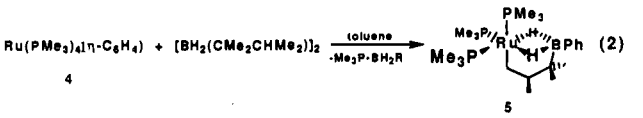

characterized further. The molecular structure of **5**, determined by X-ray diffraction (Figure 4), consists of a pseudooctahedral ruthenium center with facial PMe_3 ligands and a unique $RuC_3B(\mu\text{-}H)_2$ metallaheterocycle derived from B−C bond formation and C−H bond activation of the thexyl side chain. The Ru−P bond distance trans to the alkyl ligand (2.348(1) Å) is considerably longer than those trans to the Ru−H−B (av 2.267(1) Å), and Ru−C4 (2.170(3) Å) is shorter than the analogous Ru−C

(23) Hartwig, J. F.; Andersen, R. A.; Bergman, R. G. *Organometallics* **1991**, *10*, 1875.

(24) Statler, J. A.; Wilkinson, G.; Thornton-Pett, M.; Hursthouse, M. B. *J. Chem. Soc., Dalton Trans.* **1984**, *3*, 1731.

Table 5. $^{31}P\{^1H\}$ NMR Spectra[a]

compd		Chemical Shift in ppm (multiplicity and $^2J_{PP}$)
3a	at 100 °C	2.0 (v br, 2P), −3.9 (d tr, 234, 27), −19.4 (d tr, 234, 33)
	at −80 °C[b]	20.4 (d d d, 41, 31, 22), −1.5 (d d d, 233, 31, 25), −8.5 (d d d, 25.5, 25, 22)[c], −16.8 (d d d, 233, 41, 25.5)
3b	at 95 °C	−0.3 (d d, 32, 28), −3.8 (d tr, 230, 28), −22.9 (d tr, 230, 32)
	at −80 °C[b]	16.1 (d d d, 38, 31, 21), −1.7 (d d d, 228, 31, 26), −11.6 (d d d, 26, 25, 21)[c], −22.2 (d d d, 228, 38, 25)
3c	at 90 °C	−45.8 (d d, 23, 16, 2P), −47.4 (d tr, 209, 16) −65.5 (d tr, 209, 23)
	at −80 °C	−41.4 (br), −45.8 (d tr, 212, 16) −46.3 (br), −63.6 (d tr, 212, 25)
3d		−47.0 (d tr, 210, 17), −47.7 (ov mult), −71.6 (d tr, 210, 27)
	at −100 °C[b]	−42.1 (br mult), −43.8 (d tr, 210, 18), −46.5 (br mult), −69.6 (d d d, 210, 26, 18)
5[b]		19.0 (d d, 45.5, 17.5), 15.4 (45.5, 15), −14.4 (d d, 17.5, 15)
fac-**7**		1.4 (d d, 32, 26), −1.8 (d d, 26, 20.5), −11.0 (d d, 32, 20.5)[c]
mer-**7**		8.3 (d d, 35, 34), −2.9 (d d, 247, 35), −6.2 (d d, 247, 34)

[a] Recorded at 25 °C in toluene-d_8. [b] Recorded in THF-d_8. [c] P *trans* to Ru−H.

Table 6. DNMR Data for M−H/M−H−B Exchange in **3a−c**

compd		T_c, K	$\Delta\nu$, Hz	k_{Tc}, s^{-1}	$\Delta G^{\ddagger}_{Tc}$, kcal/mol
3a	(^{31}P)	358	3497	7767	14.7
	(^{1}H)	343	1080	2399	14.8
3b	(^{31}P)	253	3352	7445	10.6
	(^{1}H)	243	1128	2505	10.3
3c	(^{31}P)	296	593	1317	13.1
	(^{1}H)	303	1320	2932	12.9

trans-to-P bond distance (2.214(6) Å) in *cis*-RuH(Et)$(PMe_3)_4$,[18] presumably a result of steric influence of the additional phosphine ligand in the latter. The Ru−B distance (2.243(3) Å) is similar to that found in *mer*-RuH(η^2-H_2BH_2)$(PMe_3)_3$ (2.237(6) Å)[24] and considerably shorter than the Ru−B distances in the η^1-Ru−H−B moieties in **3a** (2.994(2) Å) and *fac*-**7** (2.520(3) Å, *vide infra*).

Treatment of ethylene complex Ru$(PMe_3)_4(\eta^2$-$C_2H_4)$ (**6**) with 1 equiv of 9-H-BBN dimer at −80 °C gives 1 equiv of $Me_3P{\cdot}BH(C_8H_{14})$ and colorless crystals of RuH$(PMe_3)_3[\eta^2,\eta^1$-$CH_2{=}CHB(C_8H_{14})(\mu$-H)] (**7**) which exists as a 2:1 mixture of *fac*-**7** and *mer*-**7** isomers in solution. Monitoring this reaction by multinuclear NMR spectroscopy indicated the additional formation of 9-vinyl-BBN[25] and *cis*-$RuH_2(PMe_3)_4$ (ca. 20%). Conducting the addition at 25 °C gave more of the latter products along with other unidentified ruthenium-containing products. The 9-vinyl-BBN is clearly formed by a competing reaction pathway as **7** shows no tendency to lose 9-vinyl-BBN upon heating at 100 °C. Reactions of **6** with thexylborane gave a complex mixture of products which was not characterized further.

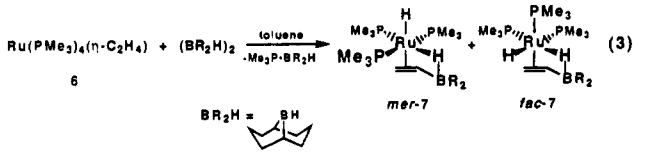

(25) Singleton, D. A.; Martinez, J. P. *J. Am. Chem. Soc.* **1990**, *112*, 7423.

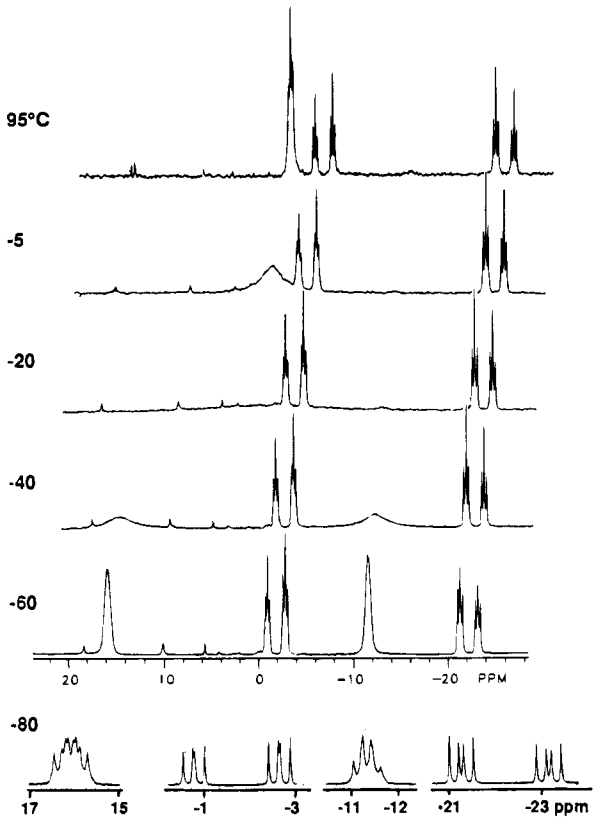

Figure 3. ^{31}P DNMR spectra of RuH$(PMe_3)_3[\eta^1,\eta^1$-$PMe_2CH_2B(C_8H_{14})$-$(\mu$-H)] (**3b**).

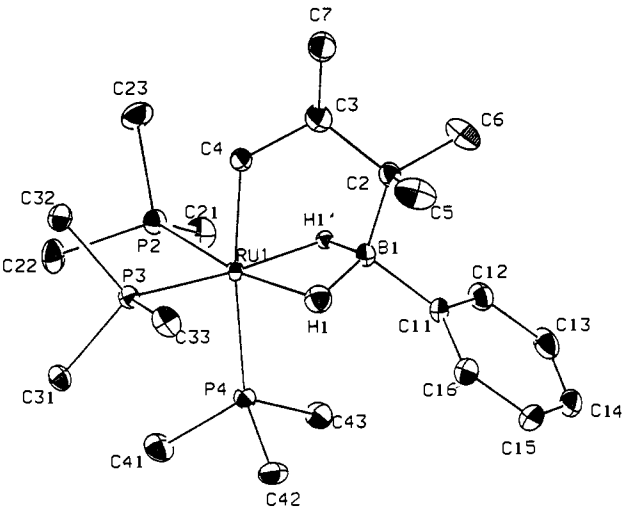

Figure 4. Molecular structure of Ru$(PMe_3)_3[\eta^1,\eta^2$-$CH_2CHMeCMe_2$-$BPh(\mu$-H)$_2$] (**5**). Hydrogen atoms are omitted for clarity.

No apparent broadening was observed in the ^{1}H or ^{31}P NMR spectra of **7** at 100 °C, indicating that both Ru−H/Ru−H−B exchange and *fac*/*mer* exchange are slow on the NMR time scale. The stereochemistry of *mer*-**7** was inferred from the singlet ^{13}C NMR resonance of the CH_2 of the vinylborane ligand; the corresponding resonance is a doublet ($^2J_{CP}$ = 12 Hz) for *fac*-**7** in which one of the PMe_3 ligands is *trans* to the coordinated vinyl group.

The molecular structure of *fac*-**7** (Figure 5), determined by X-ray diffraction, consists of a pseudooctahedral ruthenium center with facial PMe_3 ligands, an η^2-vinylborane ligand, and *cis* Ru−H and Ru−H−B moieties. The Ru−P bond distances (Table 8) are again a reflection of the *trans* ligand (Ru−P1 = 2.371(1) Å *trans* to H and Ru−P3 = 2.287(1) Å *trans* to Ru−H−B), and the Ru−C distances (av 2.256(3) Å) are significantly

Table 7. Selected Bond Distances (Å) and Angles (deg) for $Ru(PMe_3)_3[\eta^1,\eta^2\text{-}CH_2CHMeCMe_2BPh(\mu\text{-}H)_2]$ (**5**)

Ru(1)–P(2)	2.262 (1)	P(2)–Ru(1)–P(3)	94.72 (4)
Ru(1)–P(3)	2.2721 (8)	P(2)–Ru(1)–P(4)	95.41 (3)
Ru(1)–P(4)	2.3477 (8)	P(3)–Ru(1)–P(4)	96.93 (3)
Ru(1)–C(4)	2.170 (3)	P(2)–Ru(1)–C(4)	93.30 (8)
Ru(1)–B(1)	2.243 (3)	P(3)–Ru(1)–C(4)	84.61 (8)
Ru(1)–H(1)	1.763 (30)	P(4)–Ru(1)–C(4)	170.99 (8)
Ru(1)–H(1′)	1.768 (23)	P(2)–Ru(1)–B(1)	129.11 (8)
P(2)–C(21)	1.824 (3)	P(3)–Ru(1)–B(1)	132.78 (8)
P(2)–C(22)	1.832 (3)	P(4)–Ru(1)–B(1)	95.46 (8)
P(2)–C(23)	1.824 (3)	P(2)–Ru(1)–H(1)	162 (1)
P(3)–C(31)	1.826 (3)	P(2)–Ru(1)–H(1′)	95.3 (7)
P(3)–C(32)	1.829 (3)	P(3)–Ru(1)–H(1)	103 (1)
P(3)–C(33)	1.828 (3)	P(3)–Ru(1)–H(1′)	165.4 (8)
P(4)–C(41)	1.832 (3)	P(4)–Ru(1)–H(1)	84 (1)
P(4)–C(42)	1.825 (3)	P(4)–Ru(1)–H(1′)	92.8 (7)
P(4)–C(43)	1.831 (3)	C(4)–Ru(1)–B(1)	77.2 (1)
C(2)–C(3)	1.535 (4)	C(4)–Ru(1)–H(1)	87 (1)
C(2)–C(5)	1.485 (4)	C(4)–Ru(1)–H(1′)	84.1 (7)
C(2)–C(6)	1.549 (5)	B(1)–Ru(1)–H(1)	34 (1)
C(3)–C(4)	1.490 (4)	B(1)–Ru(1)–H(1′)	34.7 (7)
C(3)–C(7)	1.559 (5)	H(1)–Ru(1)–H(1′)	67 (1)
C(11)–C(12)	1.390 (4)	Ru(1)–C(4)–C(3)	114.5 (2)
C(11)–C(16)	1.386 (4)	C(3)–C(2)–C(5)	117.3 (3)
C(12)–C(13)	1.398 (5)	C(3)–C(2)–C(6)	106.1 (3)
C(13)–C(14)	1.359 (6)	C(5)–C(2)–C(6)	106.2 (3)
C(14)–C(15)	1.359 (7)	C(2)–C(3)–C(4)	112.0 (3)
C(15)–C(16)	1.392 (5)	C(2)–C(3)–C(7)	113.1 (3)
C(2)–B(1)	1.619 (4)	C(4)–C(3)–C(7)	110.2 (3)
C(11)–B(1)	1.595 (4)	C(3)–C(2)–B(1)	106.7 (2)
B(1)–H(1)	1.253 (30)	C(5)–C(2)–B(1)	109.6 (2)
B(1)–H(1′)	1.278 (23)	C(6)–C(2)–B(1)	110.9 (2)
		C(12)–C(11)–B(1)	120.8 (2)
		C(16)–C(11)–B(1)	122.8 (3)
		Ru(1)–B(1)–C(2)	114.2 (2)
		Ru(1)–B(1)–C(11)	129.9 (2)
		Ru(1)–B(1)–H(1)	52 (1)
		Ru(1)–B(1)–H(1′)	52 (1)
		C(2)–B(1)–C(11)	115.9 (2)
		C(2)–B(1)–H(1)	115 (1)
		C(2)–B(1)–H(1′)	111 (1)
		C(11)–B(1)–H(1)	105 (1)
		C(11)–B(1)–H(1′)	108 (1)
		H(1)–B(1)–H(1′)	101 (2)
		Ru(1)–H(1)–B(1)	95 (2)
		Ru(1)–H(1′)–B(1)	93 (1)

longer than those found previously for ethylene complex **6** (av 2.167(7) Å).[18]

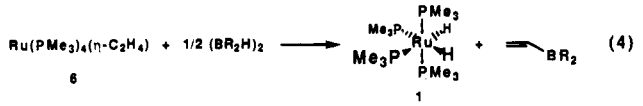

Discussion

While dihydrides *cis*-$MH_2(PMe_3)_4$ (**1**, M = Ru, Os) failed to react with both thexylborane and 9-H-BBN, addition of these hydroborating reagents to analogous d^6 monohydride complexes $MH(PMe_3)_3(\eta\text{-}CH_2PMe_2)$ (**2a,b**) was facile, giving the corresponding metallaheterocycles $MH(PMe_3)_3[\eta^1,\eta^1\text{-}PMe_2CH_2BRR'\text{-}(\mu\text{-}H)]$ (**3a–d**). In analogous reactions with rhodium- and iridium phosphine complexes, initial phosphine loss as the phosphine–borane adduct provides a vacant coordination site at the metal center for further reactions with organoboranes.[5] The absence of phosphine–borane adduct formation in this reaction, along with the observed stability of **1**, suggests that addition of organoboranes to **2** proceeds via initial electrophilic attack by boron on the CH_2 group of the Me_2PCH_2 moiety. Insertion of B–H into the M–C bond then gives the metallaheterocycles. This mechanism is in agreement with earlier reports that describe the formation of metal hydrides and

Table 8. Selected Bond Distances (Å) and Angles (deg) for $RuH(PMe_3)_3[\eta^2,\eta^1\text{-}CH_2{=}CHB(C_8H_{14})(\mu\text{-}H)]$ (**7**)

Ru(1)–P(1)	2.3714 (8)	P(1)–Ru(1)–P(2)	96.08 (3)
Ru(1)–P(2)	2.2901 (8)	P(1)–Ru(1)–P(3)	98.37 (3)
Ru(1)–P(3)	2.2869 (7)	P(2)–Ru(1)–P(3)	96.49 (3)
Ru(1)–C(9)	2.208 (2)	P(1)–Ru(1)–C(9)	112.84 (7)
Ru(1)–C(10)	2.303 (3)	P(1)–Ru(1)–C(10)	82.08 (8)
Ru(1)–B(1)	2.520 (3)	P(2)–Ru(1)–C(9)	139.74 (7)
Ru(1)–H(1)	1.553 (29)	P(2)–Ru(1)–C(10)	169.8 (1)
Ru(1)–H(1′)	1.747 (28)	P(3)–Ru(1)–C(9)	105.80 (7)
P(1)–C(11)	1.831 (3)	P(3)–Ru(1)–C(10)	93.68 (8)
P(1)–C(12)	1.823 (3)	P(1)–Ru(1)–B(1)	107.97 (7)
P(1)–C(13)	1.824 (3)	P(2)–Ru(1)–B(1)	107.60 (7)
P(2)–C(21)	1.824 (3)	P(3)–Ru(1)–B(1)	141.63 (7)
P(2)–C(22)	1.824 (3)	P(1)–Ru(1)–H(1)	176 (1)
P(2)–C(23)	1.826 (3)	P(1)–Ru(1)–H(1′)	92 (1)
P(3)–C(31)	1.824 (4)	P(2)–Ru(1)–H(1)	80 (1)
P(3)–C(32)	1.821 (4)	P(2)–Ru(1)–H(1′)	82 (1)
P(3)–C(33)	1.824 (4)	P(3)–Ru(1)–H(1)	81 (1)
C(1)–C(2)	1.533 (4)	P(3)–Ru(1)–H(1′)	169.7 (9)
C(1)–C(8)	1.537 (4)	C(9)–Ru(1)–C(10)	35.7 (1)
C(2)–C(3)	1.526 (4)	C(9)–Ru(1)–B(1)	38.26 (9)
C(3)–C(4)	1.540 (5)	C(10)–Ru(1)–B(1)	63.9 (1)
C(4)–C(5)	1.535 (4)	C(9)–Ru(1)–H(1)	71 (1)
C(5)–C(6)	1.543 (4)	C(9)–Ru(1)–H(1′)	69.7 (9)
C(6)–C(7)	1.534 (4)	C(10)–Ru(1)–H(1)	102 (1)
C(7)–C(8)	1.533 (4)	C(10)–Ru(1)–H(1′)	88 (1)
C(9)–C(10)	1.387 (4)	B(1)–Ru(1)–H(1)	75 (1)
C(1)–B(1)	1.617 (4)	B(1)–Ru(1)–H(1′)	31.9 (9)
C(5)–B(1)	1.615 (4)	H(1)–Ru(1)–H(1′)	89 (1)
C(9)–B(1)	1.577 (4)	Ru(1)–C(9)–C(10)	75.9 (2)
B(1)–H(1′)	1.389 (27)	Ru(1)–C(10)–C(9)	68.4 (1)
		Ru(1)–C(9)–B(1)	81.6 (1)
		Ru(1)–C(9)–H(9)	109 (2)
		Ru(1)–B(1)–C(1)	120.3 (2)
		Ru(1)–B(1)–C(5)	126.6 (2)
		Ru(1)–B(1)–C(9)	60.1 (1)
		Ru(1)–B(1)–H(1′)	42 (1)
		C(1)–B(1)–C(5)	106.4 (2)
		C(1)–B(1)–C(9)	118.6 (2)
		C(5)–B(1)–C(9)	118.5 (2)
		C(1)–B(1)–H(1′)	109 (1)
		C(5)–B(1)–H(1′)	101 (1)
		C(9)–B(1)–H(1′)	101 (1)
		Ru(1)–H(1′)–B(1)	106 (2)

Scheme 1

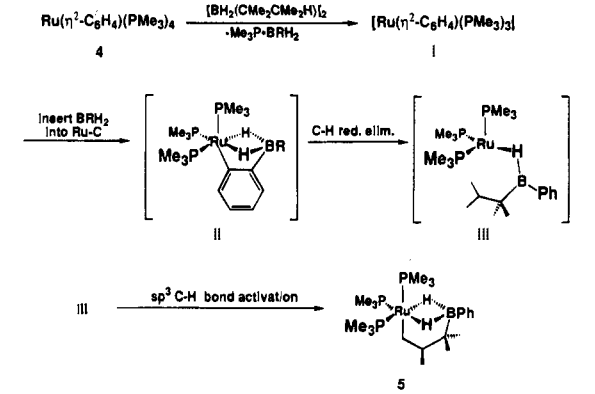

alkylboranes by addition of hydroborating reagents to saturated metal alkyl complexes.[3d,4c,d] Likewise, certain metal-catalyzed hydroborations are believed to proceed via analogous σ-bond metathesis pathways.[2e,j,4d] For **3a–d**, the newly formed organoboranes are trapped at the metal center by coordination of the P atom. Boron then coordinates to the metal via a three centered M–H–B interaction.

The facile fluxional process which equilibrates the M–H and M–H–B hydrogens and their associated *trans* PMe_3 ligands in **3a–d** can be attributed to the nature of the M–H–B bond, which can be considered not only as a B–H bond donating

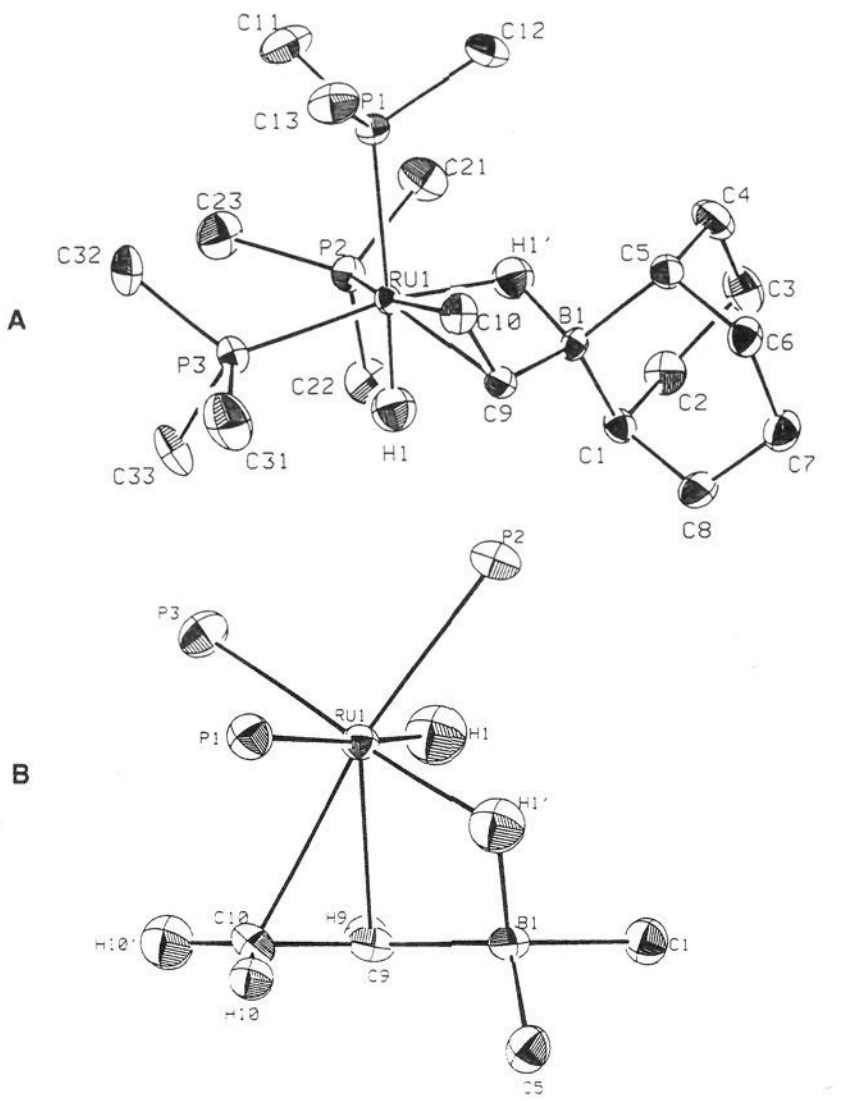

Figure 5. Molecular structure of $RuH(PMe_3)_3[\eta^2,\eta^1\text{-}CH_2{=}CHB(C_8H_{14})(\mu\text{-}H)]$ (**7**): (A) hydrogen atoms are omitted for clarity and (B) viewed along the B−C=C plane.

electron density to an unsaturated metal fragment[26] but also as an empty orbital on B interacting with the M−H bond. In this latter view of the M−H−B bond, the fluxional process observed for **3a−d** simply involves swapping the empty B orbital between the two ruthenium hydrides. Some chemical support for this view is provided by the Lewis base-mediated conversion of metal-coordinated borohydride ligands to base-borane adducts and metal hydrides.[27] The lower activation energy for exchange

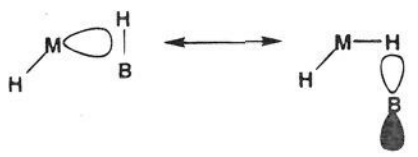

of Ru−H and Ru−H−B moieties observed for **3b** (vs **3a**) presumably reflects the weaker B−H interaction in the former which is more sterically hindered at boron. The origin of the smaller kinetic barrier for M = Os (vs Ru) is more difficult to rationalize, as the Os−H bond should be more nucleophilic than Ru−H and thus form a stronger M−H−B interaction. Perhaps the more basic Os center affords preferential charge stabilization of a transition state such as that shown below.

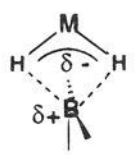

For complex **3b**, a windshield wiper-type motion of the empty boron p-orbital between the two Ru−H ligands would be sufficient to average the diastereotopic $P{-}CH_2$ (and PMe_2) resonances in the ^1H NMR spectrum. For **3a**, however, this process would not invert the asymmetric boron center. The observed equilibration of these resonances for **3a** suggests that a sequence involving dissociation of the B−H bond, rotation about the B−C bond, and formation of the new B−H bond may be occurring. If this mechanism was operative, we might expect **3a** to react with Lewis bases at boron, but no reaction was observed between **3a** and PMe_3. An alternative associative exchange mechanism involves rotation of the empty p-orbital so that overlap with both Ru−H ligands is maintained in the transition state. The "rollover" process allows rotation about the B−C bond and inversion of the asymmetric boron center.

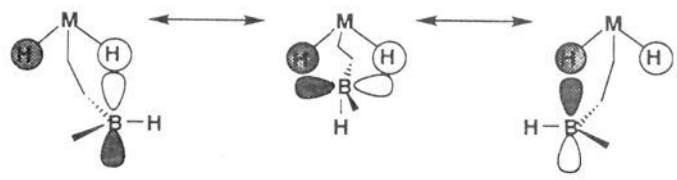

Reactions of benzyne complex **4** with protic E−H bonds usually give $RuE(Ph)(PMe_3)_4$ and/or benzene and organoruthenium products resulting from C−H bond activation.[19] The reaction of **4** with thexylborane is presumably initiated by formation of phosphine−borane and unsaturated intermediate $[Ru(PMe_3)_3(\eta^2\text{-}C_6H_4)]$ (**I**, Scheme 1). Insertion of the borane B−H bond into the Ru−C bond of the coordinated benzyne in **I** would give ruthenacycle **II**. Cleavage of the B−H bond, followed by C−H bond reductive elimination then affords ruthenium borane intermediate **III**. Oxidative addition of the C_γ−H bond of the thexyl group and reformation of the second Ru−H−B bridge then gives **5**. A similar reaction of $Cp_2Ti(\eta^2\text{-}PhC{\equiv}CPh)(PMe_3)$ with diethylborane gives phosphine−borane and the (boryl)vinyl complex $Cp_2Ti[\eta^1,\eta^1\text{-}CPh{=}CPhBEt_2(\mu\text{-}H)]$.[28]

Formation of phosphine−borane in reactions of **4** and **6** with organoboranes reflects the increased electron density at the metal center in these complexes (vs d^6 **1** and **2**) and is also observed in reactions of analogous d^8 Rh and Ir phosphine complexes.[5,6b] Further verification of this trend is provided by reaction of d^{10} $Pd(PMe_3)_4$ with organoboranes which gives only phosphine−borane and palladium metal.[29]

Reactions of organoruthenium complexes **2**, **4**, and **6** with hydridic B−H bonds bear little resemblance to those observed with protic E−H bonds, where E = NRR′,[23] OR,[23,30] SR.[30] While the latter afford addition products of the type $RuH(E)(PMe_3)_4$, borane reagents all form new B−C bonds, with the Ru−H moieties in **5** and **7** arising from C−H bond activation. This mode of reactivity is particularly relevant in the formation of vinylborane complex **7** from ethylene complex **6** as previous examples of *catalyzed* alkene borylation were proposed to involve initial insertion of the alkene into the M−B bond.[2k,7,8,31]

The reaction of **6** with 9-H-BBN provides an alternative mechanism for the borylation of alkenes. In this borylation model reaction, 1 equiv of the borane removes a PMe_3 ligand to give phosphine−borane and the unsaturated intermediate $[Ru(PMe_3)_3(\eta^2\text{-}C_2H_4)]$ (**IV**, Scheme 2). While we cannot rule out conversion of this intermediate to the (η^2-vinyl)ruthenium

(26) (a) Baker, R. T.; King, R. E.; Knobler, C.; O'Con, C. A.; Hawthorne, M. F. *J. Am. Chem. Soc.* **1978**, *100*, 8266. (b) Behnken, P. E.; Marder, T. B.; Baker, R. T.; Knobler, C.; Thompson, M. R.; Hawthorne, M. F. *J. Am. Chem. Soc.* **1985**, *107*, 932.

(27) James, B. D.; Nanda, R. K.; Wallbridge, M. G. H. *Inorg. Chem.* **1967**, *6*, 1979.

(28) Binger, P.; Sandmeyer, F.; Krüger, C.; Kuhnigk, J.; Goddard, R.; Erker, G. *Angew. Chem. Intl. Ed. Eng.* **1994**, *33*, 197.

(29) Baker, R. T., unpublished results.

(30) Burn, M. J., Ph.D. Dissertation, University of California, 1993. Burn, M. J.; Fickes, M. G.; Hollander, F. J.; Bergman, R. G. *Organometallics* **1995**, *14*, 137.

(31) Burgess, K.; van der Donk, W. A.; Westcott, S. A.; Marder, T. B.; Baker, R. T.; Calabrese, J. C. *J. Am. Chem. Soc.* **1992**, *114*, 9350.

Scheme 2

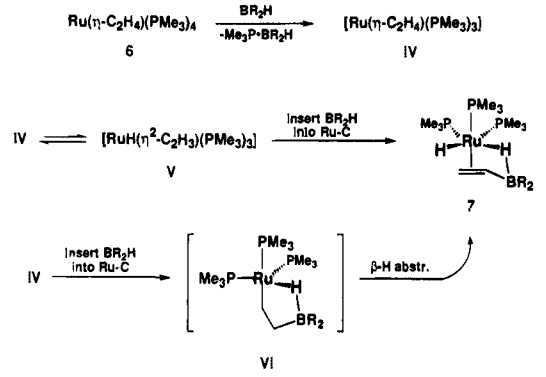

hydride (**V**),[32] followed by insertion of the borane B−H into the Ru−C bond, an alternative scheme involves initial insertion of the borane B−H into the Ru−C bond of the coordinated ethylene in **IV** to give ruthenacycle **VI** which then undergoes β-H abstraction to give **7**. Note that **VI** is analogous to Binger and Erker's cyclic titanocene derivative discussed above.[28] The ability of boryl substituents to activate adjacent C−H bonds for β-H abstraction has been observed previously for both Rh[6] and Ir[5] complexes. Smith et al. have recently reported a similar borylation reaction of 16 electron $(\eta^5\text{-}C_5Me_5)_2Ti(\eta^2\text{-}C_2H_4)$ and HBcat to give H_2 and the titanium vinylboronate ester complex, $(\eta^5\text{-}C_5Me_5)_2Ti(\eta^2\text{-}C_2H_3Bcat)$.[3f]

A third pathway for the formation of **7** invokes initial formation of **IV** followed by oxidative addition of the B−H bond to give a Ru(II)-boryl intermediate (boryl = BR_2).[33] Insertion of ethylene into the Ru−B bond with subsequent β-H abstraction would also afford (η^2-vinylborane)ruthenium hydride **7**. Indeed, vinylboronate esters are major products resulting from C−C bond insertion into Rh−B followed by β-H elimination in stoichiometric reactions of vinylarenes with $RhCl(Bcat)_2(PPh_3)_2$.[8] We consider this option less likely, however, as B−H bond activation of alkyl- and dialkylboranes (as opposed to $HB(OR)_2$) has only been observed previously for supernucleophiles such as $IrH(PMe_3)_4$.[5] In addition, increased electrophilicity of boron in 9-H-BBN (vs $HB(OR)_2$) should also favor direct B−C bond formation by electrophilic attack at carbon in the coordinated ethylene. Prior coordination of B−H to Ru in **IV** would further enhance the electrophilicity of the vacant p-orbital on boron.

In the addition of 9-H-BBN to **6** we observed a competing pathway which gave *cis*-$RuH_2(PMe_3)_4$ **1** and 9−vinyl-BBN without formation of phosphine−borane. This reaction presumably proceeds via direct electrophilic attack of the organoborane on one of the coordinated CH_2 moieties (cf. analogous reactions with **2**) to give saturated borylalkyl intermediate **VII** (Scheme 3). A similar mechanism has been invoked to explain the reaction of $(RCp)_2M(\eta^4\text{-butadiene})$ with 9-H-BBN to give the corresponding (1-boryl)allyl complex (R = H, Me; M = Zr, Hf).[34] In our case, intermediate **VII** undergoes cleavage of the Ru−H−B to give unsaturated zwitterion **VIII**, which then undergoes β-H abstraction and hydride transfer from B to Ru to give **1** and 9-vinyl-BBN.

Scheme 3

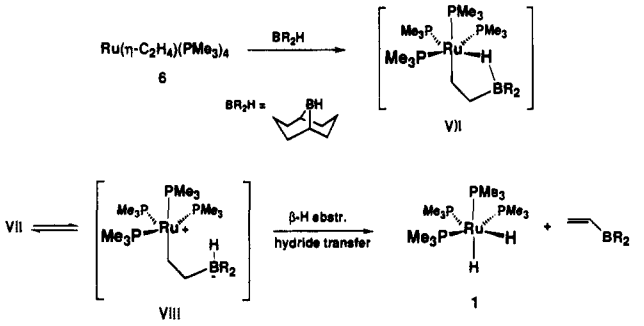

Conclusions

As found previously for organorhodium complexes,[6] reactions of organoruthenium complexes with alkylboranes proceed with formation of B−C bonds. The Lewis acidity of the resulting three-coordinate boron gives rise to Ru−H−B interactions and facile Ru−H/Ru−H−B exchange in complexes **3a−d**. The electron-rich ethylene and benzyne complexes lose PMe_3 as the phosphine−borane react with a second equiv of borane via B−C bond formation and finally form ruthenium hydrides by C−H bond activation. The borylation of Ru-coordinated ethylene via insertion of the B−H bond into the Ru−C bond suggests an alternate mechanism for catalyzed borylation[2k,7] which has been modeled previously by insertion of an alkene into an M−B bond.[8] The actual pathway taken will depend on the Lewis acidity of the borane and the basicity of the metal center.

Acknowledgment. We thank Tim Onley, Nancy Herling, Lou Lardear, Will Marshall, Laurie Howe, and Dr. Derick Ovenall for expert technical assistance, and T.B.M. thanks the Natural Sciences and Engineering Research Council of Canada (NSERC) for funding.

Supporting Information Available: Tables of final positional and thermal parameters for non-hydrogen atoms, general temperature factors, and calculated hydrogen atom positions (28 pages). This material is contained in many libraries on microfiche, immediately follows this article in the microfilm version of the journal, can be ordered from the ACS, and can be downloaded from the Internet; see any current masthead page for ordering information and Internet access instructions.

JA951109N

(32) For leading references on (η^2-vinyl)metal hydride complexes, see: Whittlesey, M. K.; Mawby, R. J.; Osman, R.; Perutz, R. N.; Field, L. D.; Wilkinson, M. P.; George, M. W. *J. Am. Chem. Soc.* **1993**, *115*, 8627. Gutiérrez, E.; Monge, A.; Nicasio, M. C.; Poveda, M. L.; Carmona, E. *J. Am. Chem. Soc.* **1994**, *116*, 791.

(33) Ruthenium boryl complexes of the type $Ru(BX_2)$, where X = heteroatom-containing substituent, have been prepared recently. Roper, W. R., unpublished results.

(34) Erker, G.; Noe, R.; Wingbermühle, D.; Petersen, J. L. *Angew. Chem., Int. Ed. Engl.* **1993**, *32*, 1213.

(35) A report on reactions of organoplatinum complexes with B_2cat_2 has recently appeared: Iverson, C. N.; Smith, M. R. III *J. Am. Chem. Soc.* **1995**, *117*, 4403.